Title
Synthesis and Characterizations of Colloidal Nanostructured Copolymers of Aniline and Aniline Derivatives

Author
GUAN, XIN NING

Publication Date
2012

Peer reviewed|Thesis/dissertation

UNIVERSITY OF CALIFORNIA

Los Angeles

Synthesis and Characterizations of Colloidal Nanostructured Copolymers of Aniline and Aniline Derivatives

A thesis submitted in partial satisfaction of the requirements for the degree Master of Science in Chemistry

by

Xin Ning Guan

2012

ABSTRACT OF THE THESIS

Synthesis and Characterizations of Colloidal Nanostructured Copolymers of Aniline and Aniline Derivatives

by

Xin Ning Guan

Master of Science in Chemistry

University of California, Los Angeles, 2012

Professor Richard B. Kaner, Chair

Nanostructured conducting polymers such as polyaniline are promising candidates for next-generation electronics because of their low cost, mechanical flexibility, good solution processability, along with the low-dimensionality that is characteristic of nanoscale materials. Here, we further expand the attractive properties of polyaniline by copolymerizing it with a variety of substituted aniline monomers, with electron donating groups, electron withdrawing groups, or substituents that can enhance the solubility of the final polymer. The resulting copolymers combine the unique properties of the homopolymers such as the high electrical conductivity of polyaniline and the good processability/solubility of the polyaniline derivatives.

Scanning electron microscope (SEM) images reveal the nanofibrous nature of the copolymers with uniform diameters. The feeding ratios of aniline and aniline derivatives of one representative copolymer are elucidated from ^{1}H-NMR studies. The different relative compositions of each copolymer also allow us to tune the electrical transport properties, the optical absorption, and the stability of the aqueous dispersion step-by-step, characterized by 2-probe resistance, UV-vis, and Zeta-potential measurements, respectively.

The resulting copolymers exhibit enhanced conductivity compared to the poorly conductive substituted-polyaniline homopolymers and better aqueous dispersion stability than their conventional bulk counterparts, rendering them suitable for many potential applications.

The thesis of Xin Ning Guan is approved.

Qibing Pei

Xiangfeng Duan

Richard B. Kaner, Chair

University of California, Los Angeles

2012

Table of Contents

Acknowledgement

I am truly thankful for the support and continual encouragement I have received from my advisor, Dr. Richard Kaner. I sincerely appreciate all the help he has provided.

I want to thank my graduate student mentor, Ms. Yue (Jessica) Wang for her support and mentorship. I am so grateful to have a knowledgeable, caring, motivating, inspirational, and friendly mentor like her.

I would also like to thank the entire Kaner Group for their guidance and contribution. I have enjoyed the time I have spent with the Kaner Group in the past two years, which is truly amazing and incredible.

I want to express my sincere thanks to Undergraduate Research Scholars Program (URSP), Litton Scholarship, Department of Chemistry and Biochemistry at UCLA for financially supporting my research. Receiving these financial supports has definitely played a major role in assisting me to achieve my academic and career goals.

I also want to thank my family for their unconditional support for the past twenty-three years.

I am extremely proud of being one of the members of the Departmental Scholars Program at UCLA, and have this extraordinary opportunity to earn my masters degree of science in chemistry.

Synthesis and Characterizations of Colloidal Nanostructured Copolymers of Aniline and Aniline Derivatives

By Xin Ning Guan

Abstract of the Thesis:

Nanostructured conducting polymers such as polyaniline are promising candidates for next-generation electronics because of their low cost, mechanical flexibility, good solution processability, along with the low-dimensionality that is characteristic of nanoscale materials. Here, we further expand the attractive properties of polyaniline by copolymerizing it with a variety of substituted aniline monomers, with electron donating groups, electron withdrawing groups, or substituents that can enhance the solubility of the final polymer. The resulting copolymers combine the unique properties of the homopolymers such as the high electrical conductivity of polyaniline and the good processability/solubility of the polyaniline derivatives.

Scanning electron microscope (SEM) images reveal the nanofibrous nature of the copolymers with uniform diameters. The feeding ratios of aniline and aniline derivatives of one representative copolymer are elucidated from ^{1}H-NMR studies. The different relative compositions of each copolymer also allow us to tune the electrical transport properties, the optical absorption, and the stability of the aqueous dispersion step-by-step, characterized by 2-probe resistance, UV-vis, and Zeta-potential measurements, respectively.

The resulting copolymers exhibit enhanced conductivity compared to the poorly conductive substituted-polyaniline homopolymers and better aqueous dispersion stability than their conventional bulk counterparts, rendering them suitable for many potential applications.

Chapter 1. Introduction:

1.1 Properties of Polyaniline

Conducting polymers are organic materials that are capable of conducting electricity. In recent years, conducting polymers have attracted tremendous amount of attention due to the great potential for many applications such as rechargeable batteries, light-emitting diodes, molecular sensors, and gas separation membranes.[1-6] Polyacetylene, polythiophene, polypyrrole, polyaniline, and many other polymers show conductance when they are doped. In order to maximize conducting polymer's commercial feasibility; they must have good solution processability and excellent chemical stability even under prolonged usage or storage. Among the family of conducting polymers, polyaniline poises as an especially attractive member due to its unique properties, which include the simple acid-base doping-dedoping chemistry, ease of synthesis and environmental stability.[7-9] However, polyaniline suffers from low solubility and poor processability in common solvents, such as water or ethanol, and can only be processed in harsh and toxic chemicals such *m*-cresol or *N*-methylpyrrolidone.

Polyaniline is a conjugated polymer that is typically synthesized by chemical oxidative polymerization with a strong oxidant in an acidic medium. The as-synthesized polyaniline tends to be in its emeraldine salt oxidation state (Figure 1.1), which is conductive ($\sigma \sim$ 1-100 S/cm) and green in color. Such a conductive emeraldine salt form can be dedoped by adding $NH_3{\cdot}H_2O$ to form an insulating emeraldine base form ($\sigma < 10^{-7}$ S/cm), which appears dark blue in color. The conductivity between the doped form and dedoped form of polyaniline can differ by over ten orders of magnitude[26]. The chemical structure of the emeraldine base state of polyaniline contains fifty percent of nitrogens in the amine form and fifty percent in the imine form with a 3:1 benzene rings-to-quinoid rings ratio. Leucomeraldine, which is the fully reduced form of

polyaniline that is white/colorless, can be produced upon reduction of the emeraldine base form, in which all aromatic rings are in the benzenoid form and connected by amine groups. Pernigraniline, the violet-colored, fully oxidized form of polyaniline, forms upon the oxidation of the emeraldine base form, with a chemical structure composed of alternating benzene rings and quinoid rings connected by imine groups.

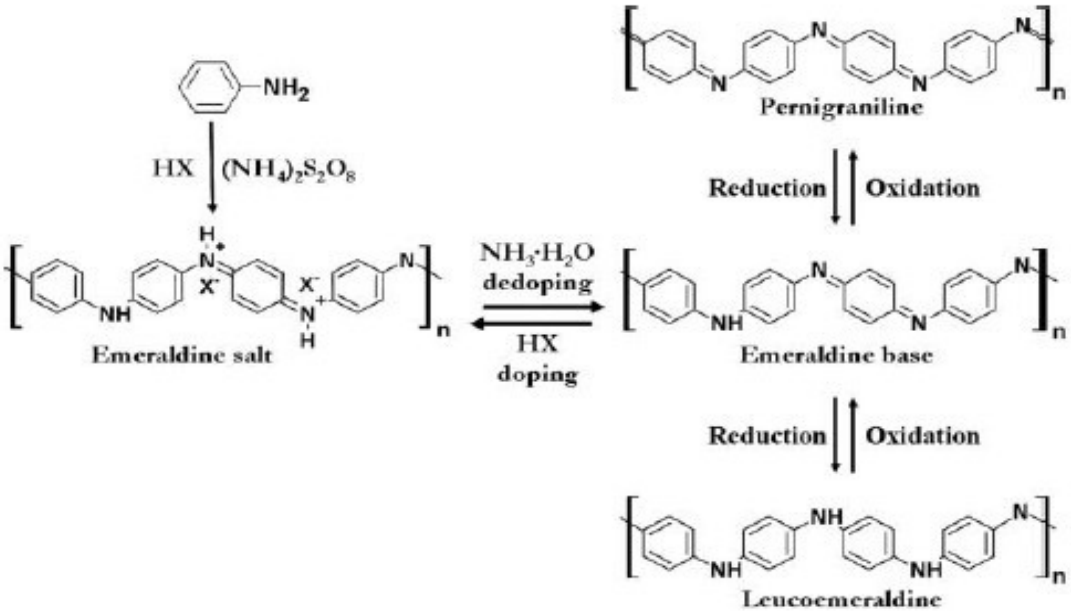

Figure 1.1 Reversible acid/base doping-dedoping properties and different oxidation states of polyaniline.[7]

1.2 Properties of Polyaniline Derivatives

In comparison to the parent polymer, polyaniline, its derivatives possess many enhanced properties such as better dispersability in organic solvents (methanol, etc.) due to the side groups, [10,11] higher resistance against microbial and chemical degradation, [12,13] and poise as an appealing alternative as charge dissipaters for e-beam lithography.[14] In addition, the different side groups in the polyaniline derivatives can offer high selectivity when used as a chemical sensor.[15]

However, the applications of polyaniline derivatives are limited due to its poor conductivity. For example, the conductivity of acid-doped poly(*o*-toluidine) is only 0.01-0.1 $S \cdot cm^{-1}$, whereas the conductivity of doped polyaniline ranges from 1 to 100 $S \cdot cm^{-1}$.[16, 17]

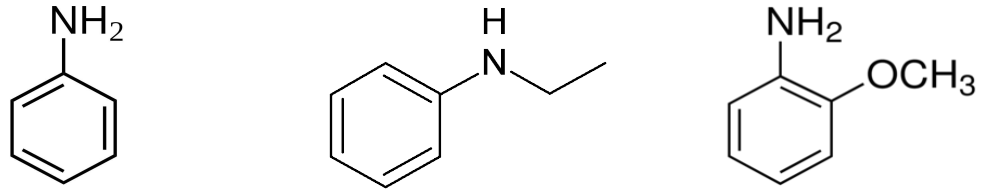

Figure 1.2 Chemical structures of aniline, *N*-ethylaniline, and *o*-anisidine.

1.3 Motivations and Purpose of Study

Combining the attractive properties of polyaniline and polyaniline derivatives is extremely desirable because the resulting copolymers can synergistically combine the benefits of both components and thus lead to a highly conductive polymer with good processability. Copolymerization can be readily achieved by incorporating both an aniline derivative and the aniline monomer in a polymerization reaction. In particular, the nanostructures of copolymers such as nanotubes, nanofibers, and nanowires are especially attractive because of their low dimensionality and high surface area.[15] Here, we report a synthetic route to nanofibers of a large variety of copolymers of polyaniline and substituted polyaniline in an effort to create a highly conductive polymer with good solubility, processability, multi-functionality, and the many attractive properties associated with 1-D nanostructures. The optical and electrical properties of the copolymers can be readily tuned by varying the relative composition. Furthermore, the nanofibrous morphology allows the copolymers to exhibit excellent colloidal stability, crucial for film processing and device fabrication.

1.4 General Template-Free Methods to Synthesize Polyaniline Nanostructures

Nanostructures of polyaniline such as nanorods, nanofibers, nanowires, and nanotubes have been synthesized via different physical and chemical methods. Examples of physical methods for synthesizing polyaniline nanostructures include mechanical stretching[19] and electrospinning.[18] However, these polyaniline syntheses have only been carried out on a small scale. Chemical methods such as template-assisted polymerization with nanoporous membranes [20-22] or addition of structural directing molecules such as surfactants [23] of bulky dopant acids have faced several difficulties, for example, the inability to remove the templates or side products in order to recover the nanostructure during the post-synthetic treatment.

Recently, a number of template-free methods have been reported including interfacial polymerization, rapid mixing of reactants, dilute polymerization, electrochemical polymerization on conducting substrates, sonochemical [41] and radiolytic-assisted syntheses.[42] The resulting nanofibers have enabled improved performances in many applications ranging from chemical sensors, supercapacitors, memory devices, and actuators.

Our group has pioneered two synthetic routes, interfacial polymerization and rapidly mixed polymerization, which leads to high purity polyaniline nanofibers with small diameters. [24, 25] Nanofibers with diameters less than 100 nm and as small as 30 nm have been successfully synthesized [26] which are among the smallest reported without using a template. [27]

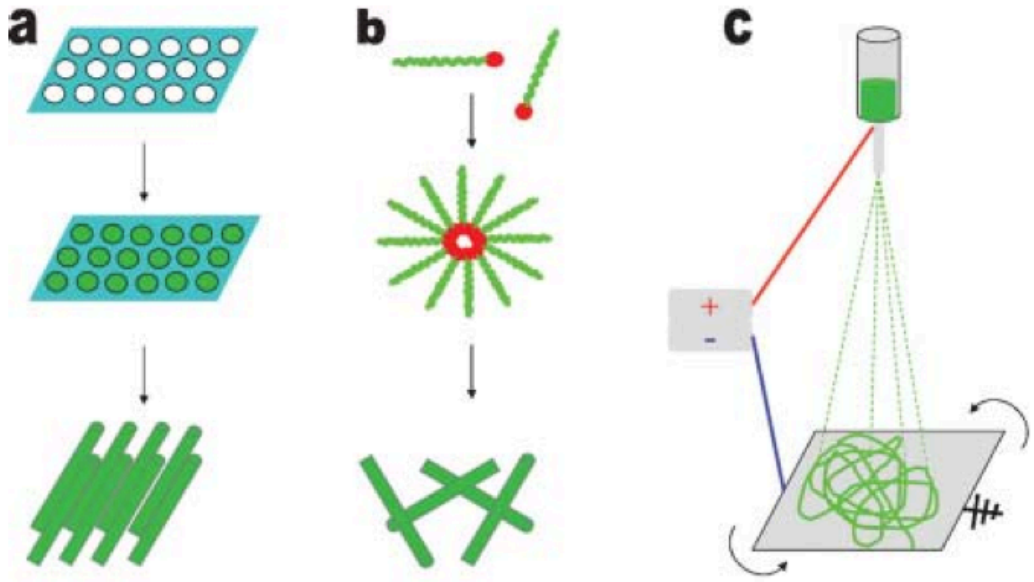

Figure 1.4 Different routes to produce polymer nanostructures: (a) template-assisted, (b) structural directing using surfactants, (c) electrospinning. [26]

1.4.1 Interfacial Polymerization

Interfacial polymerization yields the formation of polymer at the interface of an immiscible aqueous and organic biphasic system,[33] in a fashion similar to the synthesis of Nylon. Our lab has developed this synthetic strategy towards polyaniline nanofiber production (Figure 1.4.1). Aniline monomer is dissolved in an organic solvent while a strong oxidant (APS) is placed in an aqueous acidic phase; formation of polyaniline initiates at the interface and slowly diffuses into the aqueous layer. [27, 24, 34] Diffusion of the newly formed polyaniline into the water layer is due to the poor solubility of the as-produced polyaniline in organic media, since it is in the emeraldine salt oxidation state, it is positively-charged and hydrophilic. [26] Interfacially polymerized polyaniline shows a nanofiber structure with average fibril diameters between 30-50 nm. [26] The aniline monomer, initiator, and oxidant only meet at the interface and react to form polyaniline nanofibers. The diffusion of the as-produced polyaniline nanofibers into the aqueous

phase prevents the secondary growth of the nanofibers to form agglomerates, which is formed in conventional polymerization routes; and leaves the interface available for continuous nanofiber formation. [26]

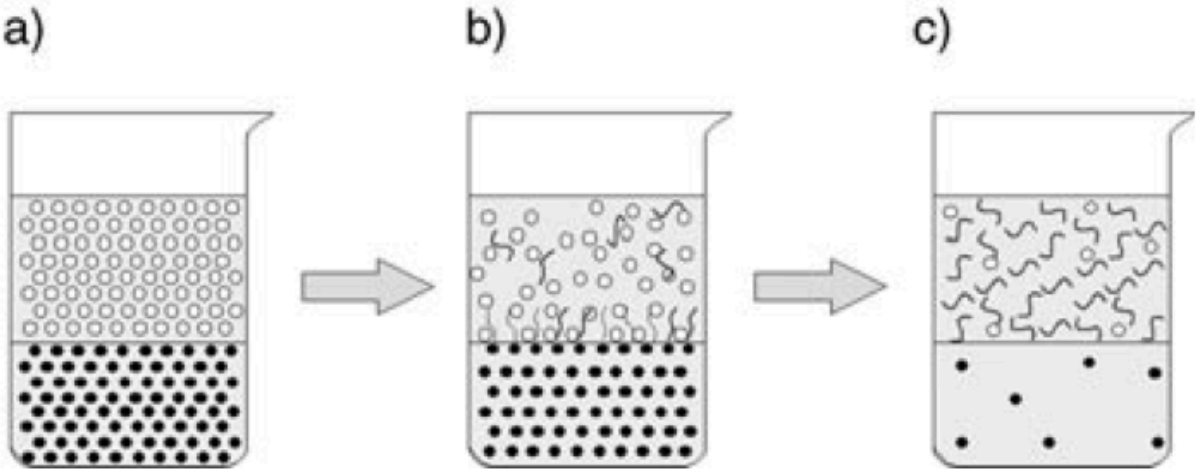

Figure 1.4.1 Interfacial polymerization for polyaniline nanofibers (a) interface is set up between an organic phase containing dissolved aniline (solid circles) and an aqueous phase containing the oxidant, (b) formation at the interface, (c) diffusion of as-produced polyaniline into the water layer. [25]

1.4.2 Initiator-Assisted Rapid Mixing Polymerization

More recently, our lab has developed the initiator-assisted rapid mixing polymerization method, which was used in our copolymerization experiments (Figure 1.4.2). [28] Addition of an initiator such as *p*-phenylenediamine (benzenediamine) or 1,4-benzenediamine (aniline dimer) to a rapidly mixed reaction is the key. Such a polymerization method leads to a noticeably enhanced reaction rate and the formation of nanofibers is further favored as the initiator radicals serve as homogeneous nucleation sites for growing polymer chains. [28] Polymers that are synthesized via a rapid mixed polymerization with a small amount of initiator show relatively

small diameters, which is also tunable by varying the doping acid. [28] The resulting nanofibers can be cast into homogeneous and porous films, which are useful for devices like sensors. However, the electronic properties including response time and sensitivity of the devices can be further improved if the aspect ratio of the polyaniline nanofibers can be enhanced. This can be achieved by increasing the length of the polyaniline nanofibers while holding the diameter constant. Our group were able to produce polyaniline nanofibers as long as >30 μm with diameters as small as roughly 36 nm by improving the reaction conditions such as by changing the aniline monomer to oxidant molar ratio with different concentration of initiators. [28]

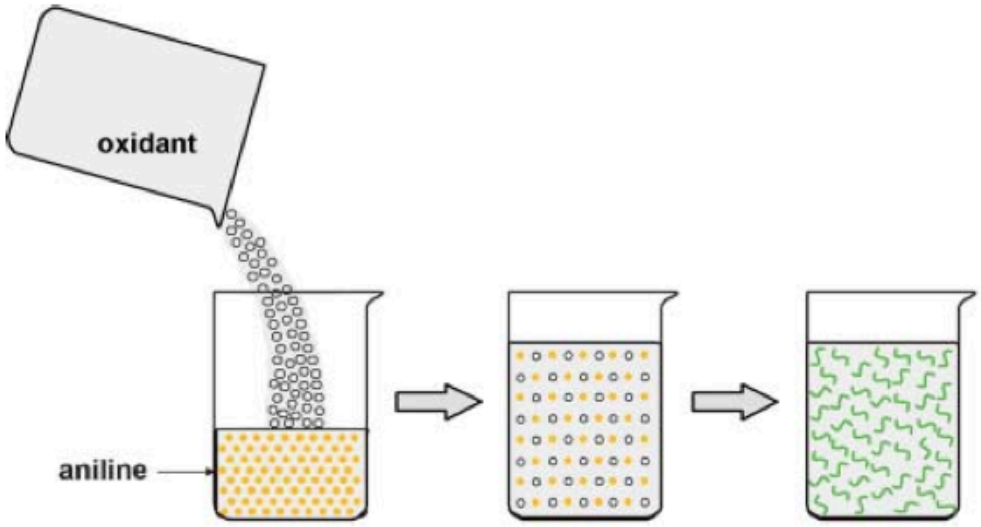

Figure 1.4.2 Schematic illustration of rapid mixing polymerization. [28]

Chapter 2. Experimental

2.1 Materials

Aniline was purchased from Acros Organic. *N*-ethylaniline, *o*-Anisidine, *N*-phenyl-1,4-phenylenediamine, 98% (*p*-dimer) were purchased from Aldrich Chemical Co. Ammonium peroxydisulfate (APS) and hydrochloric acid (12.1M) were bought from Fisher Scientific Co.

Deuterated dimethyl sulfoxide (DMSO-d_6) was purchased from Cambridge Isotope Laboratories, Inc. All chemicals were used without further purification.

2.2 Synthesis of Copolymers of Aniline and *N*-ethylaniline at Different Ratios via Initiator-Assisted Rapid Mixing Copolymerization

To synthesize copolymers of aniline and aniline derivatives, aniline monomer and *N*-ethylaniline monomer with different relevant ratios were added in 10 mL of 1 M HCl in a 20 mL scintillation vial. 500 µl of 0.007 M of *N*-phenyl-1, 4-phenylene-diamine (*p*-dimer) dissolved in methanol was added to this solution. In a separate container, 0.18 g of ammonium peroxydisulfate (APS) was dissolved in 10 mL of 1 M HCl. These two fresh made solutions were rapidly mixed and vigorously shaken for about 10 seconds to promote mixing, and the mixed solution was left undisturbed for one day. [26] The nanofibers were purified by dialysis (dialysis tube, 12000-14000 MW cutoff, Fisher Scientific) against deionized water for approximately one day to remove reaction byproducts and low molecular weight impurities. The resulting purified copolymers were collected and stored in 20 mL scintillation vials at room temperature. The reactions were initiated by *N*-phenyl-1,4-phenylene-diamine (*p*-dimer) in this set of copolymerization. Table 2.2 shows the feeding compositions in the copolymerization of aniline and *N*-ethylaniline at different ratios.

Ratio (Ani. Deri. Vs. Ani.)	*N*-ethylaniline (µL)	Aniline (µL)	*p*-dimer (mg)	Solvent 1: 1M HCl (mL)	APS (g)	Solvent 2: 1M HCl (mL)
10:0	403	0	3.5	10	0.18	10
9:1	321.6	25.9	3.5	10	0.18	10
8:2	294.2	53.3	3.5	10	0.18	10
7:3	265.2	82.3	3.5	10	0.18	10
6:4	234.4	113.1	3.5	10	0.18	10
5:5	201.5	146	3.5	10	0.18	10
4:6	166.6	180.9	3.5	10	0.18	10

3:7	129.2	218.3	3.5	10	0.18	10
2:8	89.2	258.3	3.5	10	0.18	10
1:9	46.2	301.3	3.5	10	0.18	10
0:10	0	292	3.5	10	0.18	10

Table 2.2 Synthesis of copolymers of *N*-ethylaniline and aniline at different ratios

2.3 Preparation of Samples for Characterization

Microscopy. Scanning electron microscopy (SEM) samples were prepared by drop-casting doped copolymer nanofiber dispersions onto silicon wafers, and air-drying for one day. SEM images were collected on a JEOL JSM-6700-F filed emission SEM microscope.

Nuclear Magnetic Resonance (NMR). For ^{1}H-NMR sample preparation, the purified copolymer nanofibers were dedoped by dialyzing against 0.1 M $NH_3{\cdot}H_2O$ for one day followed by another day in deionized water. The dedoped copolymer dispersions were centrifuged at 3,500 rpm to remove most of the solvent, and the products were dried in a 60 °C vacuum oven overnight and cooled down at room temperature. The dried nanofibers were dissolved in deuterated dimethyl sulfoxide (DMSO-d_6) followed by filtration through quartz wool to remove the solid debris. NMR spectra were collected on a Bruker ARX400 spectrometer.

UV-vis Spectroscopy. The nanofiber aqueous dispersion samples were prepared by diluting 500 μL of the purified copolymer dispersion in 3 mL deionized water for UV-vis absorption measurements. All spectra were taken on an HP 8452 spectrometer.

Conductivity Measurements. 2 mL of purified copolymer nanofiber dispersions were drop-cast onto a clean glass slide, and air-dried for 2 days. Silver paste was used to define electrodes that are approximately 2 mm apart. The current-voltage (I-V) curves were measured on a standard probe station. The film thicknesses were measured with a Dektak 6 Surface Profile

Measuring System. Conductivity values were calculated from the slope of the I-V curves and the thickness of the corresponding films.

Zeta-Potential Measurements. 400 μL of purified copolymer dispersion was diluted to 40 mL with a 0.01 M HCl solution to obtain a final pH of 2. The pH of the dispersion was varied by the addition of 1 M NaOH solution. The zeta-potential values of the dispersions were measured in disposable folded capillary cells (DTS10601) with a Malvern Nano-ZS ZEN-3600 Zetasizer in Zeta mode.

Chapter 3. Discussion and Characterizations

3.1 Morphological Characterization

A large number of substituted anilines have been polymerized with aniline to form copolymer nanofibers by rapidly mixing the reactants in the presence of an initiator. In a typical reaction, upon the addition of the oxidant solution to the solution containing the initiator and equivalent molar amount of the two monomers, the reaction mixture turns from clear to light blue/violet within a few seconds, indicating the formation of the pernigraniline oxidation state. [15] The mixture rapidly gets darker in color as the reaction progresses and eventually becomes deep green when collected after 1 day, characteristic of the conducting emeraldine salt oxidation state. In contrast, control reactions carried out under identical conditions, but without an initiator, progress at a much slower rate, often taking hours before a noticeable color change and as long as days before solid precipitation occurs. SEM analyses reveal a drastic difference between the morphologies of the copolymers produced without and with an initiator. Copolymers synthesized in the absence of an initiator are generally granular in morphology.

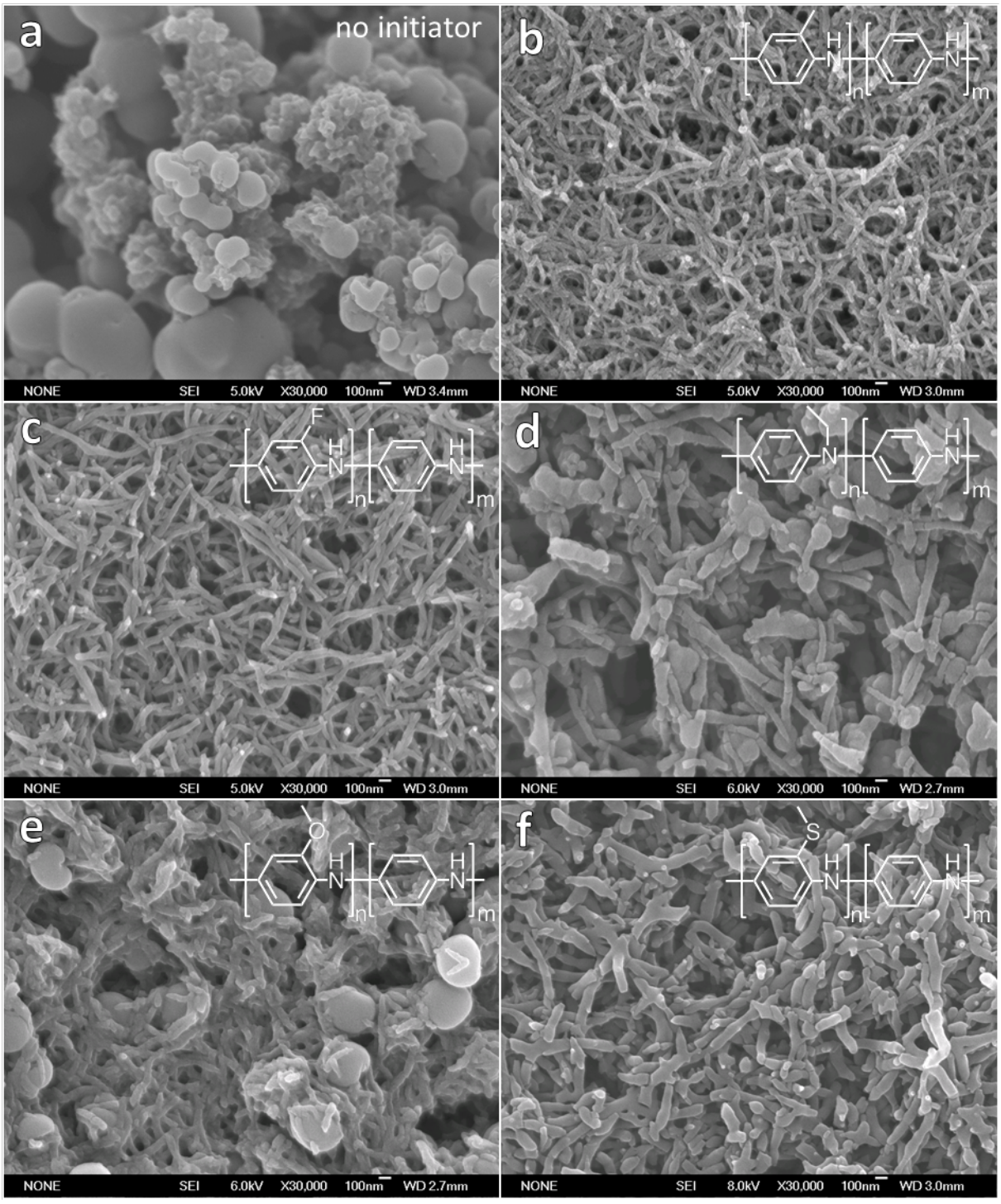

Figure 3.1.1 SEM images of a) a copolymer produced without an initiator, and b-f) with an initiator: b) poly(aniline-*co*-*o*-toluidine), c) poly(aniline-*co*-2-fluoroaniline), d) poly(aniline-*co*-*N*-ethylaniline), e) poly(aniline-*co*-*o*-anisidine), f) poly(aniline-*co*-2-(methylthio)aniline).

Figure 3.1.1a shows a typical SEM image for a copolymer synthesized without an initiator, in which case no nanofibers were formed due to steric and electronic factors.[29] On the other hand, in the presence of an initiator, homogeneous nucleation is preferred due to the faster rate of reactive nuclei formation, which promotes nanofibrous structure rather than agglomeration caused by heterogeneous nucleation.[28] By adding aromatic initiators such as *N*-phenyl-1,4-phenylene-diamine (*p*-dimer), or *p*-phenylenediamine (*p*-diamine), which have much lower oxidation potentials than the aniline derivative monomers, into the solutions, the polymerization of polyaniline derivatives can be sped up considerably.[30] The rapid reaction rate suppresses secondary growth that leads to agglomeration, and therefore promotes the formation of nanofibers of polyaniline derivatives. Nanofibers appear as the preferred morphology for the parent polyaniline even without the addition of an initiator. Hence, as we optimize the synthetic conditions to promote the growth of polyaniline derivative 1-D structures, nanofibers of the copolymer of polyaniline and different substituted polyaniline building blocks can be obtained under similar reaction parameters.

Using the initiator-assisted approach, mats of continuous nanofiber networks become the dominant morphology for the polymerization product. Copolymer nanofibers have been obtained at a 50/50% aniline/aniline derivative feeding ratio for copolymers containing strongly electron donating substitutes including poly(aniline-*co*-*o*-anisidine), poly(aniline-*co*-2-(methylthio)aniline), strongly electron withdrawing substituents such as poly(aniline-*co*-2-fluoroaniline), poly(aniline-*co*-3-fluoroaniline), poly(aniline-*co*-4-fluoroaniline), poly(aniline-*co*-3,4-difluoroaniline), poly(aniline-*co*-2-chloroaniline), poly(aniline-*co*-3-chloroaniline), alkyl groups substituted on the aromatic ring including poly(aniline-*co*-*o*-toluidine), poly(aniline-*co*-*m*-toluidine), and alkylated amine groups such as poly(aniline-*co*-*N*-ethylaniline). Figure 3.1.1

b-f illustrates the morphology of five representative copolymers with their structures shown in the upper right corner. Some spheres are observed in poly(aniline-*co*-*o*-anisidine) shown in Fig. 3.1.1e, but nanofibers still remain as the main morphology. The average diameter for these nanofibers ranges from ~50 nm to 300 nm and lengths ~300 nm to 2 μm depending on the aniline derivative involved.

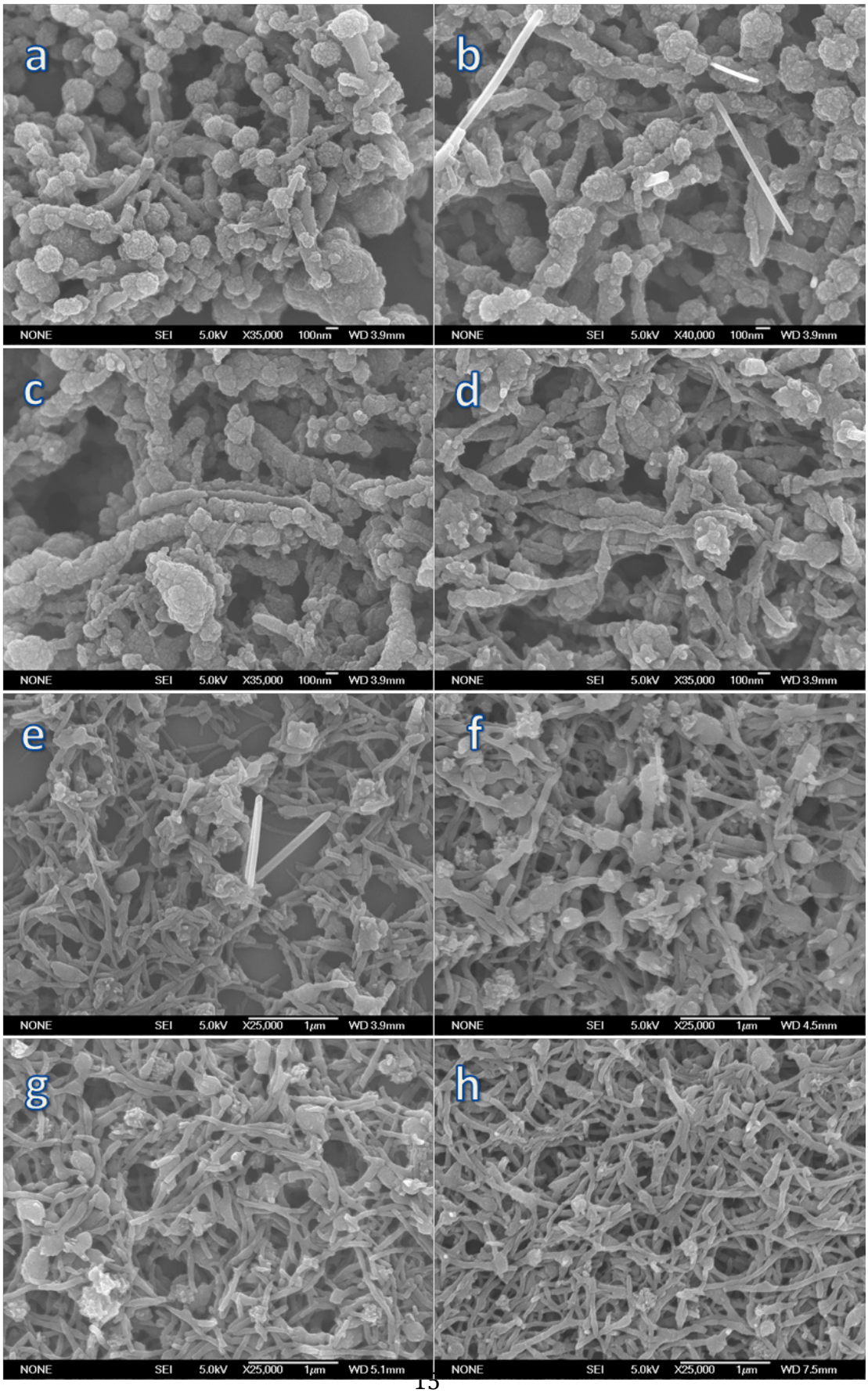
a
NONE SEI 5.0kV X35,000 100nm WD 3.9mm
b
NONE SEI 5.0kV X40,000 100nm WD 3.9mm
c
NONE SEI 5.0kV X35,000 100nm WD 3.9mm
d
NONE SEI 5.0kV X35,000 100nm WD 3.9mm
e
NONE SEI 5.0kV X25,000 1μm WD 3.9mm
f
NONE SEI 5.0kV X25,000 1μm WD 4.5mm
g
NONE SEI 5.0kV X25,000 1μm WD 5.1mm
h
NONE SEI 5.0kV X25,000 1μm WD 7.5mm

Figure 3.1.2 SEM images of copolymers of aniline and *N*-ethylaniline at different ratios (ratio of *N*-ethylaniline vs. aniline), a) 9:1, b) 8:2, c) 7:3, d) 6:4, e) 5:5, f) 4:6, g) 3:7, h) 2:8.

In order to examine the effect of the relative aniline/substituted aniline feeding composition on the final copolymer morphology, copolymers of aniline and *N*-ethylaniline with different relative ratios were synthesized and examined by SEM (Figure 3.1.2). As the ratio of aniline to *N*-ethylaniline increases, the morphology of the resulting copolymers steadily transitions from mostly granular to mostly nanofibrous. This phenomenon demonstrates that nanofibers are intrinsic to polyaniline, agreeing with previous reports.[26] In a monomer mixture that contains both aniline and an aniline derivative, the overall reaction rate is slowed down as the reaction rates for substituted polyanilines are slower than that for the parent polymer as a result of both steric and electronic effects, which lead to an agglomerated morphology for the final copolymer. At a 5:5 aniline-to-*N*-ethylaniline feeding ratio, nanofibers become the dominant structure for the resulting copolymer (Fig. 3.1.2e), while very few spheres were observed when the aniline feeding ratio was increased to 80% (Fig. 3.1.2h).

3.2 Compositional Characterization

In the synthesis of copolymers of aniline and aniline derivatives with an initiator at different ratios, the compositions of aniline and aniline derivatives were determined by integrating ^{1}H-NMR peak areas in each copolymer. The reactivity ratios, block copolymers of aniline r_1, and *N*-ethylaniline r_2 can be calculated via copolymer composition equation. [31]

$$\frac{(1-2F_1)f_1}{(1-f_1)F_1} = r_2 + r_1\frac{f_1^2(F_1-1)}{(1-f_1)^2F_1}$$

where F_1 is the molar composition of the aniline derivative in the copolymer, and f_1 is the aniline derivative in the monomer feed mixture. The ability of a monomer to react in copolymerization,

which depends on the factors of steric, resonance stabilization, and polarity of the monomer, could determine the reactivity ratios.[32] Due to this characterization, we could actually calculate the reactivity of both monomers and design a specific ratio of these starting materials, to develop a desired final copolymer composition.

In order to study the polymerization kinetics, we use poly(aniline-*co*-*N*-ethylaniline) synthesized at various aniline to *N*-ethylaniline ratios as an example to demonstrate the relationship between the monomer feeding ratio and the actual copolymer composition.

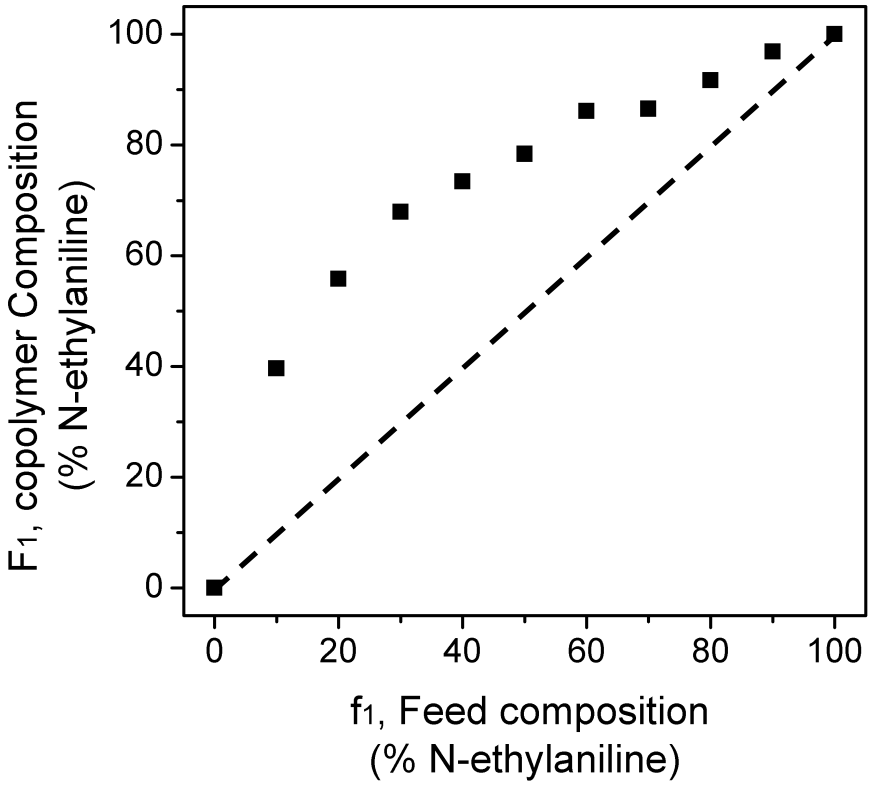

Figure 3.2 Feeding composition of *N*-ethylaniline.

The molecular structure of poly(aniline-*co*-*N*-ethylaniline) is shown as the inset in Fig. 3.1.1d. The compositions of the relative ratio between the two repeat units can be calculated by taking the ratio of the integrated ^{1}H-NMR peak areas of the CH_3 methyl proton (δ = 1.04 ppm) to

the aromatic resonance peaks at around 6.5-7.5 ppm. The actual molar composition of *N*-ethylaniline, denoted as F_1, is plotted against f_1, the feeding composition of *N*-ethylaniline as shown in Figure 3.2. The diagonal dashed line represents equal composition of the two constituents, in which case this suggests identical reactivity.

In Figure 3.2, the trend of the data points are not linear, but above the diagonal line. For example, when the starting ratio of the copolymer of aniline and *N*-ethylaniline is 5:5, the actual composition of *N*-ethylaniline in the resulting copolymer only contains around 78% of the *N*-ethylaniline. Therefore, it can be concluded that *N*-ethylaniline is more reactive than aniline. Steric factors, resonance stabilization, and polarity of the monomers dictate the ability of a monomer to react in copolymerization. The electron donating nature of the ethyl substituent on the amine group is likely to stabilize the cation free radical intermediates during the polymerization, thus attributing to its higher reactivity. Hence, when equal amounts of the monomers are present in the reaction mixture, a higher composition of *N*-ethylaniline than aniline is obtained for the final copolymer. This result agrees with previous studies on other copolymer system such as poly(aniline-*co*-*o*-ethylaniline) and poly(aniline-*co*-*N*-butylaniline). Therefore, the addition of an initiator has dramatic effects on the reaction rate and the product supramolecular morphology, but not the reactivity of the monomers.

3.3 Optical Absorption Characterization

To study the relationship between composition and optical properties of the resulting copolymers of aniline and *N*-ethylaniline, UV-vis (HP 8453 spectrometer) measurements were carried out.

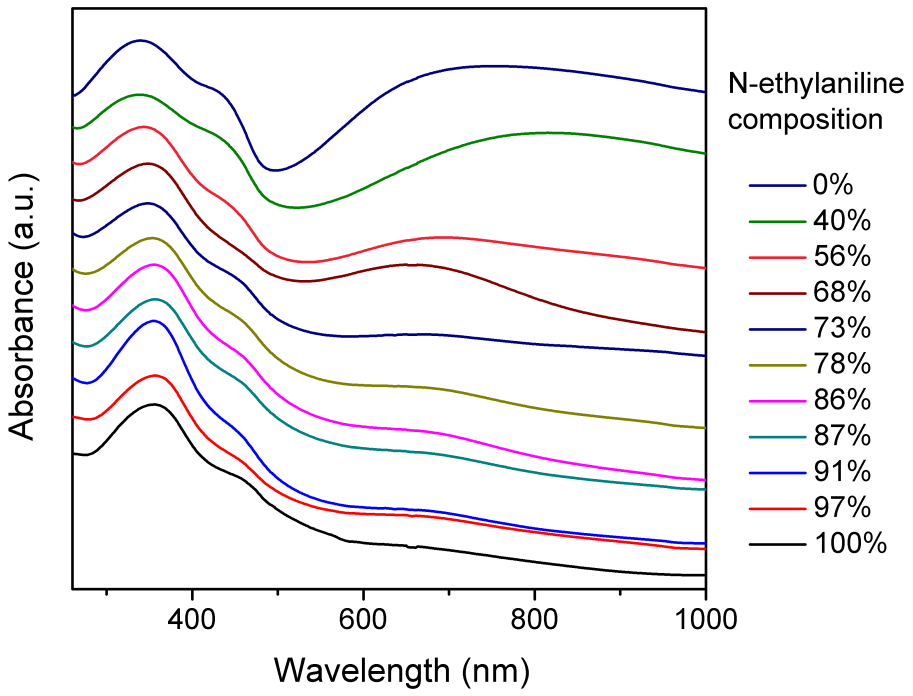

Figure 3.3.1 Normalized UV-vis spectra of copolymers of aniline and *N*-ethylaniline with increasing *N*-ethylaniline content from 0%-100%.

The normalized UV-vis plot is shown in Figure 3.3.1 with *N*-ethylaniline composition labeled in the legend. Three peaks are observed for all copolymers appearing at around 340 nm, 440 nm, and 680 nm. A strong peak around 340 nm can be assigned to the π-π^* transition[35]. As the ratio of *N*-ethylaniline increase, the absorption peaks shift to higher wavelength. For example, the π-π^* peak appears at 360 nm for poly(*N*-ethylaniline) and gradually decreases as the aniline composition increases and approaches that of polyaniline at 333 nm. The bathochromic shift could be due to the weaker intermolecular interactions as a less ordered chain conformation of the resulting copolymers form.[36] The polyaniline homopolymer shows a broad peak at around 600 nm. As the N-ethylaniline content increases, the broad peak becomes weaker and weaker and a hypsochromic shift is observed. The poly(*N*-ethylaniline) shows a very weak peak at around 650 nm. The hypsochromic shift suggests a higher π-polaron band transition

energy, which is likely the result of the steric effect of the *N*-ethyl side group, leading to more chain twisting and thus decreased conductivity. [37-40]

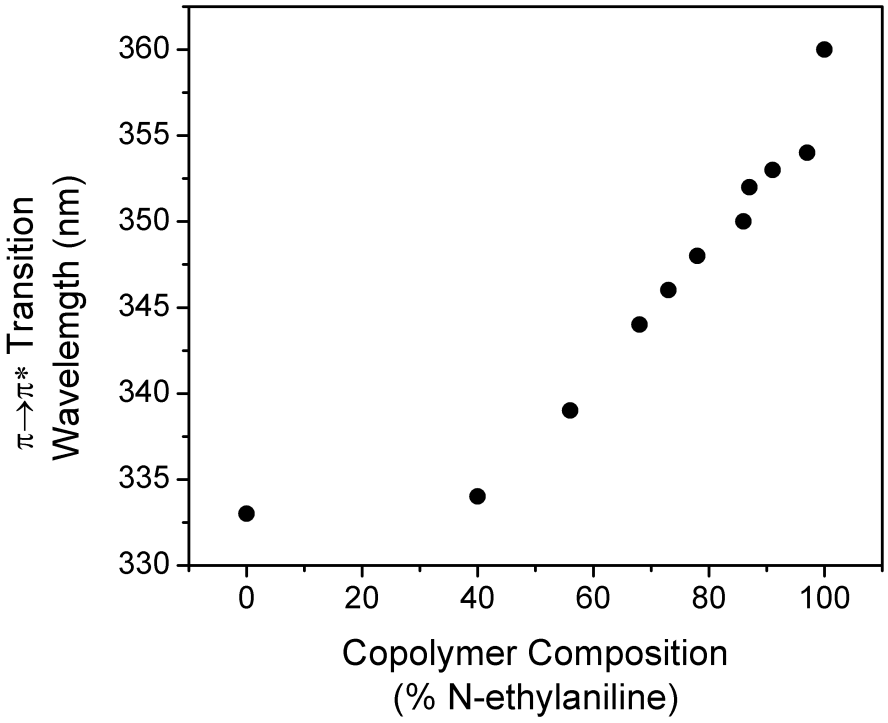

Figure 3.3.2 π-π^* peak transition with different compositions of copolymers.

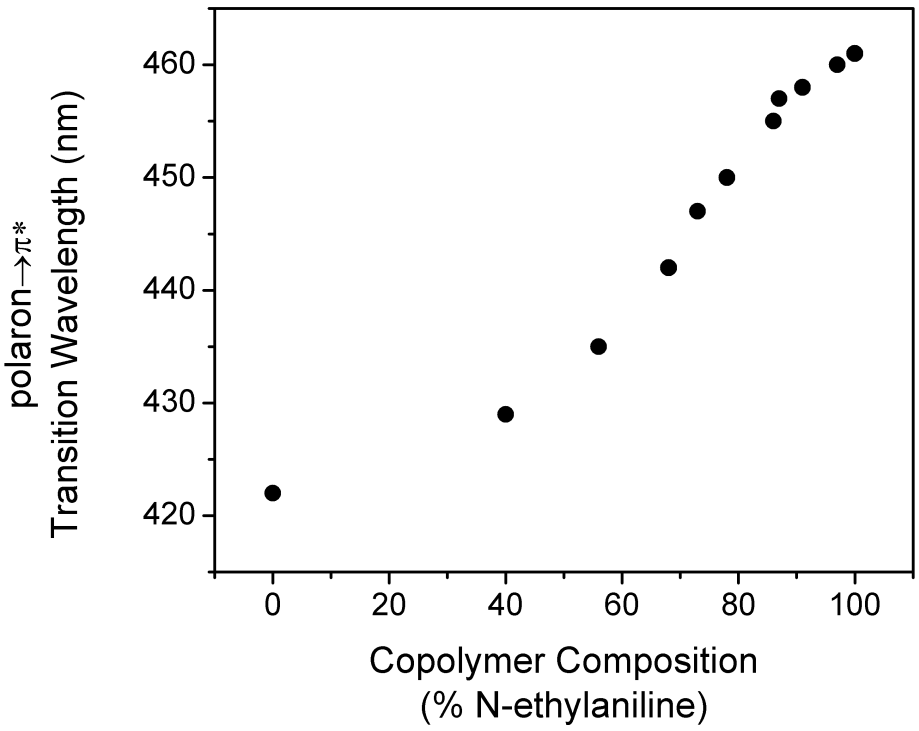

Figure 3.3.3 Polaron-π* transition with different composition of copolymers.

The peak positions for the copolymers with different compositions are plotted in Figure 3.3.2. A pseudo-linear relationship is observed, illustrating the stepwise variation in copolymer composition. A similar trend is observed when analyzing the polaron- π* transition as peak shifted from 461 nm for poly(*N*-ethylaniline) to 422 nm for polyaniline in a close to linear relationship with respect to the varying in composition (Figure 3.3.3).

3.4 Electrical Characterization

Conductivity measurements of the copolymers were carried out via a two-probe method at room temperature. The copolymer solutions were drop-cast on top of a clean glass slide. The concentration of the copolymer solutions was adjusted to optimize the film uniformity and surface smoothness. When the copolymer solution is too concentrated, the film cracks during the drying process, which yields little to no macroscopic electrical conductivity due to the

discontinuity of the films. Once a smooth and uniform film was obtained, silver paint was pasted on the film surface approximately 2 μm apart serving as electrodes. As previously mentioned, polyaniline derivatives have poor electrical conductivity due to the steric and electronic effects of the side groups. Hence, it is not surprising that the conductivity of poly(*N*-ethylaniline) is poor and has the highest sheet resistance among the thin films with different polyaniline to poly(*N*-ethylaniline) building block ratios.

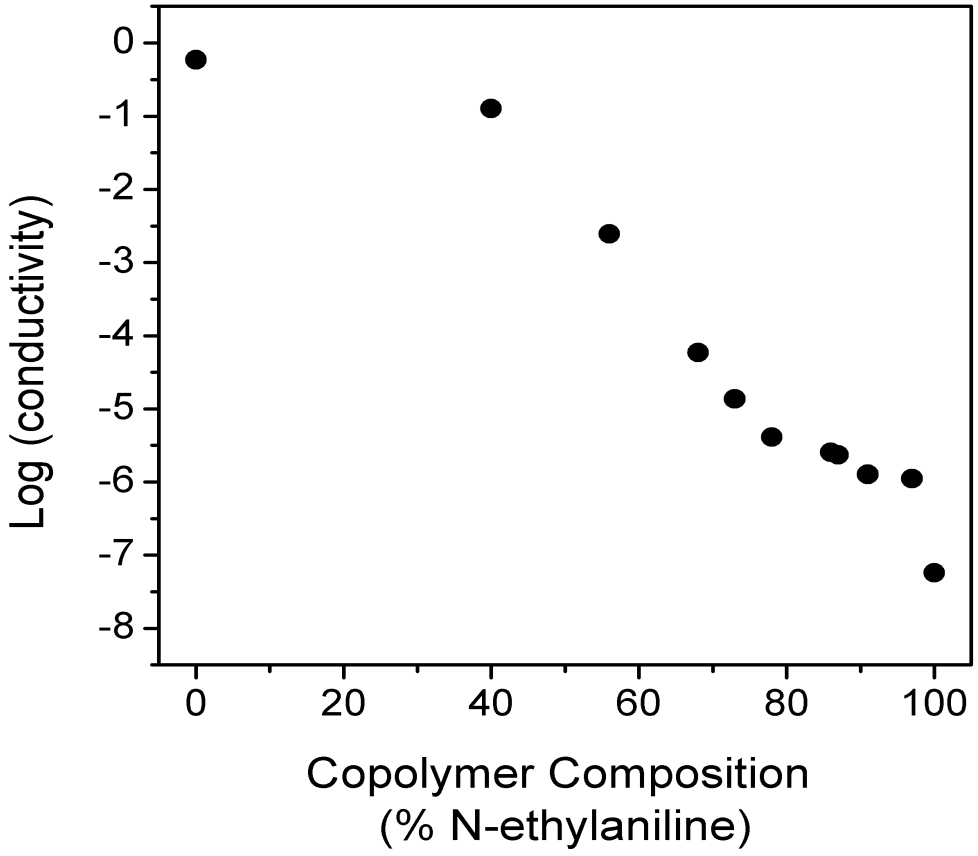

Figure 3.4 Conductivity of the copolymers of aniline and *N*-ethylaniline at different *N*-ethylaniline compositions.

Table 3.4 Conductivity of the copolymers of aniline and *N*-ethylaniline at different feeding *N*-ethylaniline compositions

% Ethyl (final composition)	Conductivity (S/cm)	log(conductivity)
100	5.73E-08	-7.24
97	1.12E-06	-5.95
91	1.27E-06	-5.90
87	2.34E-06	-5.63
86	2.54E-06	-5.60
78	4.13E-06	-5.38
73	1.37E-05	-4.86
68	5.88E-05	-4.23
56	0.00247	-2.61
40	0.127	-0.896
0	0.589	-0.230

The conductivities of polyaniline derivatives tend to be lower than that of the parent polymer. We found that the doped poly(*N*-ethylaniline) nanofibers have a conductivity of 5.7×10^{-8} S/cm, similar to a reported value of 1.3×10^{-7} S/cm. However, the conductivity increased by two orders of magnitude with just 7% of polyaniline in the copolymer composition, plotted in log scale in Figure 3.4 and tabulated in Table 3.4. The conductivity further increases steadily as the content of polyaniline gets higher, and becomes on the same order of magnitude as the polyaniline nanofibers with a 40% poly(*N*-ethylaniline) composition. The conductivity only increases slightly from 0.13 to 0.59 S/cm as the poly(*N*-ethylaniline) building block decreases from 40% to 0%, which suggests a percolation threshold is reached around a composition of 60% polyaniline. Therefore, the conductivities of the copolymers can be readily tuned over a seven orders of magnitude range by varying their composition.

3.5 Colloidal Stability Characterization

Polyaniline nanofibers can form a lyophobic colloidal dispersion in low pH aqueous conditions because of the electrostatic repulsion from the positively charged polymer backbone.

[38] Such properties are desirable for device fabrication because smooth, uniform films can be readily obtained via simple techniques such as drop-casting. Here, we employ zeta potential measurements, which provide useful information about the stability of a colloidal system, to assess the surface charges on the copolymer nanofibers in order to acquire a semiquantitative understanding of the copolymer nanofiber colloidal stability.

All zeta potential measurements were carried out incrementally from pH 2 to 12 in order to minimize the formation of salt and electric double layer compression in strongly acidic environment (i.e. below pH 2). The zeta potential values of polyaniline are not only affected by the $\{[H^+] / [OH^-]\}$ ratio of the aqueous solution, but also the extent of doping/dedoping. Generally, the zeta values of polyaniline increase with increasing $[H^+]$; however, when $[H^+] \geq 10^{-2}$ M, the zeta values decrease with increasing $[H^+]$ due to the compression of electric double layer resulting from the high ionic strength. Therefore, all of the zeta measurements were carried out at pH 2-12 to reduce the amount of salt formation and to avoid the electric double layer compression in strong acidic environments.

3.5.1 Zeta-Potential Measurements of Polyaniline, Poly(*N*-ethylaniline), and Poly(aniline-*co*-*N*-ethylaniline)

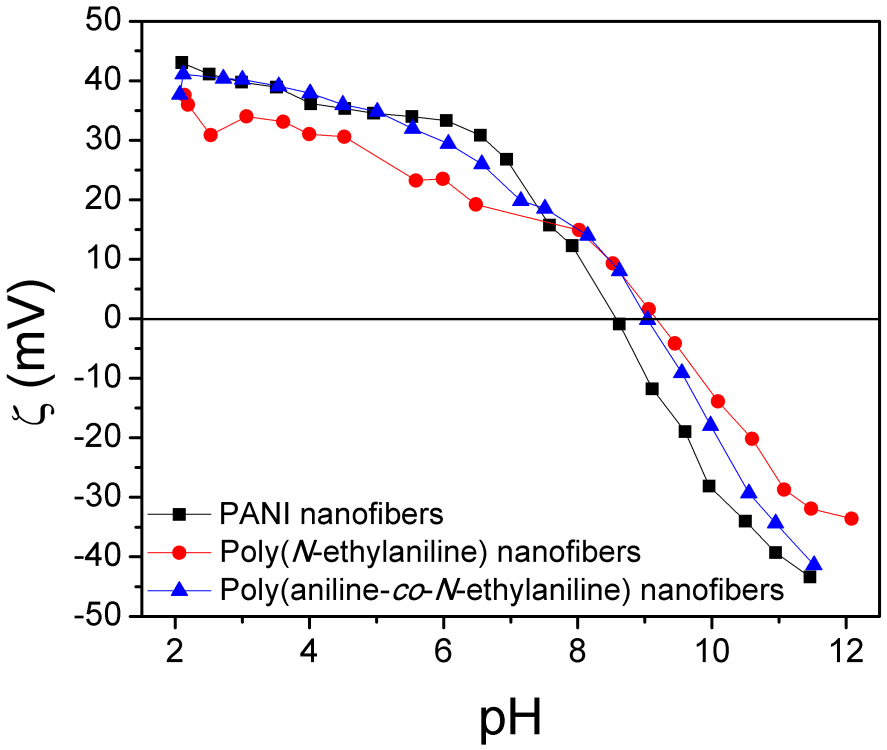

Figure 3.5.1 The zeta potential vs. pH plot for polyaniline nanofibers, poly(*N*-ethylaniline) nanofibers, and poly(aniline-*co*-*N*-ethylaniline) nanofibers.

In an acidic environment, polyaniline and substituted polyanilines are in the doped form with their backbones carrying positive charge, leading to positive zeta potential values. The polymers get dedoped in basic conditions and carry negative zeta potential values instead. A stronger electrostatic repulsion is indicated by a higher absolute value of the zeta potential, which suggests a more stable colloidal system that is more resilient to particle aggregation and precipitation. For polyaniline, a maximum zeta value of 40.9 mV is reached at pH = 2. The zeta potential decreases slowly but remains above 30 mV, above which is considered a stable colloid, until pH = ~6.4 (Figure 3.5.1). Dedoping of polyaniline occurs around this pH and the zeta values start to drop more significantly, evidenced by the steeper slope. The isoelectric point (IEP) is reached at a pH of ~8.2. The polyaniline is neutral in charge at this point, leading to a

zeta potential of 0 mV, suggesting that the electrostatic repulsion between particles is small which then tend to aggregate into larger particles. The zeta potential values continue to decrease as the pH is further lowered until it reaches its minimum at -41.6 mV at pH = 12.

The zeta potential vs. pH plot for poly(*N*-ethylaniline) nanofibers are also shown in Fig. 3.5.1. A peak zeta potential value of 38.1 mV is reached at pH = 2, lower than that of polyaniline at the same pH, and the zeta potential remains above 30 mV until the pH is increased to ~4.5, indicating poly(*N*-ethylaniline) nanofibers have a narrower colloidal stability pH range. This is possibly due to the fact that the ethyl substituent on the amine and imine nitrogens are shielding some of the positive charges on the polymer backbone. However, the IEP is reached at a higher pH value of 9.1 for the poly(*N*-ethylaniline) nanofibers compared to that of polyaniline. The weakly electron donating effect of the ethyl group on the nitrogen gives poly(*N*-ethylaniline) a higher pKa value than the parent polymer. Therefore, the positive charges on its backbone do not get completely neutralized until a more basic pH.

To study the effect of copolymerization on the colloidal stability, the copolymer with a 20% *N*-ethylaniline feeding composition is chosen as it yields a final copolymer with a close to 1:1 polyaniline to poly(*N*-ethylaniline) composition. The zeta potential curve of the resulting copolymer nanofiber, shown in Fig. 3.5.1, illustrates a similar peak zeta potential of 41.1 mV at pH = 2 similar to polyaniline. The zeta potential value stays in the 30 mV and above range until pH = ~6.0, much higher than that of poly(*N*-ethylaniline) nanofibers, while approaching the 6.4 pH value from polyaniline. This trend clearly demonstrates the significance of copolymerization as at approximately equal parent polymer to polyaniline derivative composition, the good colloidal stability is extended to a broader pH range. Furthermore, the IEP of the copolymer

occurs at pH = 9.0, only slightly lower than that of poly(*N*-ethylaniline) and much higher than that of polyaniline.

3.5.2 Zeta-Potential Measurements of Polyaniline, Polyethylaniline, Poly(aniline-*co*-ethylaniline)

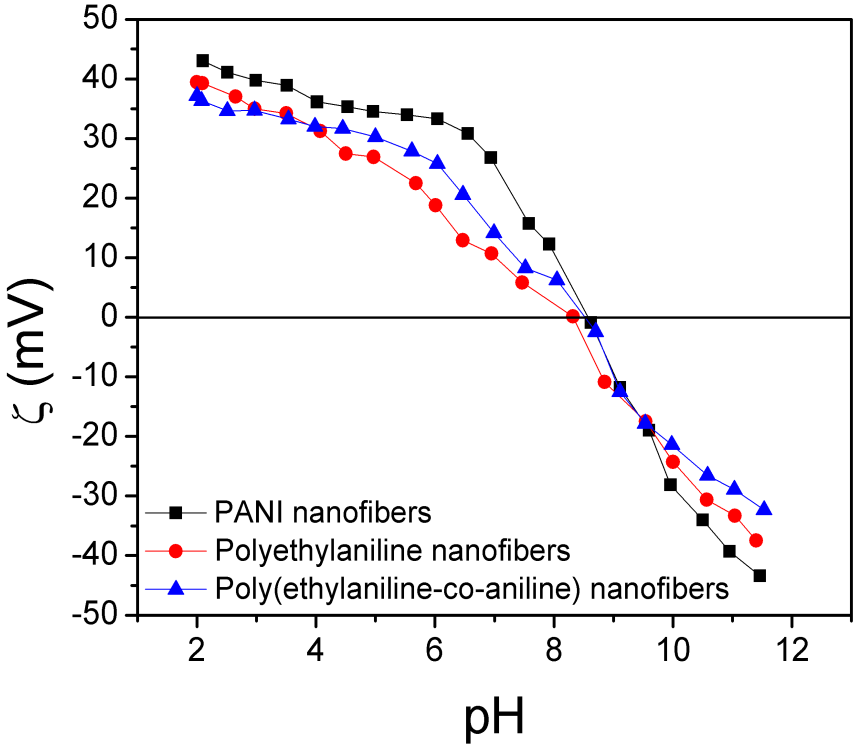

Figure 3.5.2 The zeta potential vs. pH plot for polyaniline nanofiber, polyethylaniline nanofibers, and poly(aniline-*co*-ethylaniline) nanofibers.

The colloidal stability of poly(aniline-*co*-ethylaniline) is also analyzed and compared to polyaniline and the corresponding substituted polyaniline. A maximum zeta value of 43.03 mV for polyaniline is observed in Figure 3.5.2. The maximum zeta potential value of poly(aniline-*co*-ethylaniline) is the lowest among these three polymers, but it is very close to polyethylaniline. A peak zeta potential value of 39.47 mV is reached at pH = 2, lower than that of polyaniline at the same pH, and the zeta potential remains above 30 mV until the pH reaches around 4. In

comparison to the resulting copolymer, a peak value of 37.17 mV is observed at pH = 2, and the zeta potential remains above 30 mV until the pH reaches around 5.4. This phenomenon indicates polyethylaniline has a narrower colloidal stability pH range compared to its copolymer. The colloidal stability and stable pH window of poly(aniline-*co*-ethylaniline) falls in-between those of polyaniline and polyethylaniline, demonstrating that the incorporation of polyaniline building blocks into polyethylaniline improves its colloidal stability. In addition, these three polymers have a very similar IEP around pH = 8.6, which also suggests that the weak electron donating effect of the ethyl group on the aromatic rings has very little effect on the pK_a of polyethylaniline and the corresponding copolymer.

3.5.3 Zeta-Potential Measurement of Polyaniline, Polychloroaniline, Poly(aniline-*co*-chloroaniline)

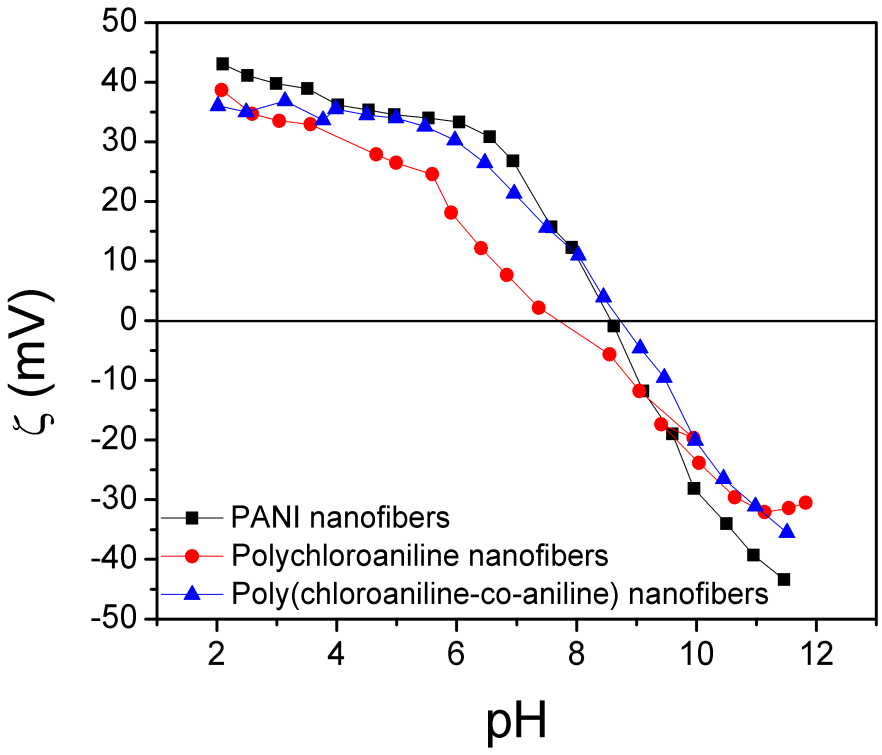

Figure 3.5.3 The zeta potential vs. pH plot for polyaniline nanofibers, polychloroaniline nanofibers, and poly(aniline-*co*-chloroaniline) nanofibers.

Maximum zeta potential values of polychloroaniline and poly(aniline-*co*-chloroaniline) are 38.67 mV and 36.03 mV, respectively. These two values are lower than the polyaniline maximum zeta potential value, as expected. The zeta potential remains above 30 mV for polychloroaniline until the pH is increased to around 4.2. And the zeta potential remains above 30 mV for its copolymer until the pH is increased to around 6.5, which is close to the polyaniline colloidal stability pH range. Through this observation, we believe that the polychloroaniline blocks of the copolymer have significant impact on the colloidal stability. The Cl side group is a strong electron-withdrawing group, which reduces the electron density on the polymer backbone and hence leads to a lower pK_a for the polymer. Therefore, the IEP of polychloroaniline appears at pH = 7.8, much lower than that of polyaniline and poly(aniline-*co*-chloroaniline) at pH ~9. Such evidence again illustrates the enhancement in colloidal stability by copolymerization.

Chapter 4 Conclusion

4.1 Summary

We have demonstrated the successful synthesis of nanostructured copolymers of aniline and aniline derivatives via an initiator-assisted rapid mixing polymerization. Morphological studies of the resulting copolymers suggest that nanofibers are more likely to form as the polyaniline composition increases. The addition of an initiator can accelerate the copolymerization rate, which is essential for nanofiber formation. Compositional studies reveal that aniline derivatives have higher reactivities compared to aniline due to the inductive effects of their side groups. The relationship between the feeding and actual compositions of a series of a representative copolymer, poly(aniline-*co*-*N*-ethylaniline), is obtained via ^{1}H-NMR studies.

Optical absorption studies via UV-vis spectroscopy demonstrate a pseudo-linear trend in the shifting of absorption peak positions for copolymers with different compositions. Electrical characterization reveals that as the content of aniline increases in the copolymer, the conductivity of the resulting copolymer increases, reaching a percolation threshold and reaching the same order of magnitude as the polyaniline nanofibers at a 40% poly(*N*-ethylaniline) composition. Zeta potential results quantify the relationship between composition and colloidal stability of the doped dispersions for polyaniline, substituted polyaniline, and the resulting copolymers. The data show that the colloidal stability pH range of poly(aniline-*co*-*N*-ethylaniline) is close to the polyaniline pH range, while poly(*N*-ethylaniline) has a much narrower colloidal stability pH range. Therefore, copolymerization of aniline and an aniline derivative into nanofibrous forms synergistically combine the benefits of the parent polymer and the substituted polymer, leading to enhanced aqueous colloidal stability and improved, tunable electrical properties. Combined with the versatile functionalities that the various substituents bring, these copolymer nanofibers could be suitable for a broad range of applications such as chemical sensors, supercapacitors and organic electrodes.

References

1. Skotheim, T. J. Ed. *Handbook of Conducting Polymers,* Dekker; New York, **1986**; Vols. 1 and 2.
2. Anderson, M. R.; Mattes, B. R.; Reiss, H.; Kaner, R. B. *Science,* **1991**, 252, 1412.
3. Liang, W. B.; Martin, C. R. *Chem. Mater.,* **1991**, 3, 390.
4. Gustafsson, G.; Cao, Y.; Treacy, G. M.; Klavetter, F.; Colaneri, N.; Heeger, J. *Nature,* **1992**, 357, 477.
5. Grem, G.;Leditzky, G.; Ullrich, B.; Leising, G. *Adv. Mater.,* **1992**, 4, 36.
6. Bartlett, P. N.; Birkin, P. R. *Synth. Met.,* **1993**, 61, 15.
7. Huang, W. S.; Humphrey, B. D.; MacDiarmid, A. G. *J. Chem. Soc., Faraday Trans. 1*, **1986**, 82, 2385-2400.
8. MacDiarmid, A. G.; Chiang, J. C.; Halpern, M.; Huang, W. S.; Mu, S. L.; Somasiri, N. L. D.; Wu, W. Q.; Yaniger, S. I. *Mol. Cryst. Liq. Cryst.,* **1985**, 121, 173-180.
9. MacDiarmid, A. G. *Synth. Met*., **1997**, 84, 27-34.
10. Gruger, A.; Novak, A.; Regis, A.; Colomban, J. *J. Mol. Struct.,* **1994**, 328, 153-167.
11. Yang, S. M.; Chiang, J. H. *Synth. Met*., **1991**, 41, 761-764.
12. Kwon, A. H.; Conklin, J. A.; Makhinson, M.; Kaner, R. B. *Synth. Met*., **1997**, 84, 95-96.
13. Cihaner, A.; Onal, A. M.; *Eur. Polym. J*., **2001**, 37, 1767-1772.
14. Angelopoulos, M.; Shaw, J. M.; Kaplan, R. D.; Perreault, S. *J. Vac. Sci. Technol*. B, **1989**, 7(6), 1519.
15. Tran, H. D.; Norris, I.; D'Arcy, J. M.; Tsang, H.; Wang, Y.; Mattes, B. R.; Kaner, R. B. *Marcromolecules,* **2008**, 41, 7405-7410.
16. Wei, Y.; Hariharan, R.; Patel, S. *Macromolecules,* **1990**, 23, 758.

17. Yoon, H.; Jung, B. M.; Lee, H. *Synth. Met.,* **1991**, 41-43, 699.

18. He, H. X.; Li, C. Z.; Tao, N.J. *Appl. Phys. Lett.,* **2001**, 78, 811-813.

19. MacDiarmid, A.G.; Jones, W. E.; Norris, I. D.; Gao, J,; Johnson, A. T.; Pinto, N.J.; Hone, J.; Han, B.; Ko, F.K.; Okuzaki, H.; Llaguno, M. *Synth. Met.,* **2001**, 119, 27-30.

20. Martin, C.R. *Acc. Chem. Res.,* **1995**, 28, 61-68.

21. Wang, C.W.; Wang, Z.; Li, M.K.; Li, H.L. *Chem. Phys. Lett.,* **2001**, 341, 431-434.

22. Wang, Z.; Chen, M.A.; Li, H.L. *Mater. Sci. Eng.,* A **2002**, 328, 33-38.

23. Yu, L.; Lee, J.I., Shin, K.W.; Park, C.E.; Holze, R. J. *Appl. Polym. Sci.,* **2003**, 88, 1550-1555.

24. Huang, J.; Kaner, R.B. *J. Am. Chem. Soc.*, **2004**, 126, 851-855.

25. Huang, J.; Kaner, R.B. *Angew. Chem., Int. Ed.*, **2004**, 43, 5817-5821.

26. Huang, J.; Kaner, R.B. *Chem. Commun.*, **2005**, 367-376.

27. Huang, J.; Virji, S.; Weiller, B.H.; Kaner, R.B. *J. Am. Chem. Soc.,* **2003**, 125, 314.

28. Tran, H.D.; Kaner, R.B. *Chem. Commun.*, **2006**, 3915-3917.

29. Mattoso, L. H. C.; Manohar, S. K.; MacDiarmid, A. G.; Epstein, A. J. *J. Polym. Sci., Part A: Polym. Chem*., **1995**, 33, 1227-1234.

30. D'Aprano G.; Lecler, M.; Zotti, G. *Synth. Met*., **1996**, 82, 59-61.

31. MacDiarmid, A. G., Chiang, J. C., Richter, A. F., Somarsiri, N. L. D., Epstein, A. J., Alacer, L., Eds. *Conducting Polymers*; Residel Publishing Co.: Dordrecht, Holland, **1987**; 105.

32. Paniter, P. C.; Coleman, M. M. *Fundamentals of Polymer Science*; Technomic Publishing Co.: Lancaster, PA, **1994**; 113.

33. Wittbecker, E. L.; Morgan, P. W. *J. Polym. Sci. Part A: Pilym. Chem*., **1996**, 34, 521-529.

34. Huang, J. X.; Virji, S.; Weiller, B. H.; Kaner, R. B. *Chem. –Eur. J.*, **2004**, 10, 1314-1319.

35. Wei, W.; Force, W. W.; Wnek, G. E.; Ray, A.; MacDiarmid, A. G. *J. Phys. Chem*., **1989**, 93, 495.

36. Roy, B. C.; Gupta, M. D.; Bhoumik, L.; Ray, J. K. *Synth. Met*., **2002**, 130, 27.

37. Li, X. G.; Zhou, H. J.; Huang, M. R. *Polymer*, **2005**, 46, 1523-1533.

38. MacDiarmid, A. G.; Epstein, A. *J. Synth. Met.,* **1995**, 69, 85.

39. Briseno, A. L.; Mannsfeld, S. C. B.; Lu, X. M.; Xiong, Y. J.; Jenekhe, S. A.; Bao, Z. N.; Xia, Y. N. *Nano Lett.,* **2007**, 7, 668.

40. Li, X. G.; Zhou, H. J.; Huang, M. R. *J. Polym. Sci. Part A: Polym. Chem.,* **2004**, 42, 6109-6124.

41. Jing, X. L.; Wang, Y. Y.; Wu, D.; Qiang, J. P. Sonochemical Synthesis of Polyaniline Nanofibers *Ultrason. Sonochem.* **2007,** 14, 75-80.

42. Pillalamarri, S. K.; Blum, F. D.; Tokuhiro, A. T.; Story, J. G.; Bertino, M. F. Radiolytic Synthesis of Polyaniline Nanofibers: A New Templateless Pathway *Chem. Mater.* **2005,** 17, 227-229.